CHINESE JOURNAL OF GEOPHYSICS Vol.48, No.5, 2005, pp: 1069~1077

STATISTIC ANALYSIS OF TROPICAL CYCLONE IMPACT ON THE CHINA MAINLAND DURING THE LAST HALF CENTURY

WANG Jin-Bo QIAN Wei-Hong

Department of Atmospheric Sciences, Peking University, Beijing 100871, *China*

Abstract The typhoon best track data provided by Joint Typhoon Warning Center (JTWC) was employed to analyze the temporal-spatial variability of the landfall tropical cyclones over the China mainland, which generated over the Northwest Pacific (NWP) basin and the South China Sea (SCS) for the period 1945~2002. Seasonally, landfall cyclones concentrated in June-November from the NWP are more than that in June-September from the SCS. Along the China coast line, the highest landfall frequency of cyclones is located in the southeast coast (27°N, 120°E) and the frequency rapidly decreases north to it. The interannual variability shows that the annual total sum of landfall cyclones is proportional to that coming from the SCS. The wavelet analysis shows that the annual series of landfall cyclone frequency has apparent spatial differentiation and temporal variations of 2~7 years. Long-term linear trends indicate that the generation frequency of cyclone over the NWP and the SCS, as well as landfall cyclone frequency in China increase at different rates. On the other hand, a short-term trend shows that decreasing trends of generation frequency and landfall frequency were observed in recent years. The short-term trend implies that there are decadal variations in generation frequency and landfall frequency. Three transition points of the decadal variations appeared around 1960, 1970, and 1990, respectively.

Key words Tropical cyclone, Interannual-decadal variation, South China Sea, Northwest Pacific, Statistic analysis.

1 INTRODUCTION

The tropical cyclones (TC) are one of the most devastating natural disasters causing tremendous loss of life and damage by extreme weather events such as gale, rainstorm and storm surge in the world. China is one of the countries which suffer the damage from TC most severely, because it adjoins the North-West Pacific (NWP) and South China Sea (SCS), over which the TCs are generated most frequently in the whole world ocean basins. The long coast line causes the discrepancy of TC landfall frequency in the areas of different latitudes. Therefore, to roundly review the spatial and temporal variations of TC formation and landfall will be helpful for understanding how TC activity varies.

Numerous studies have been made focusing on how NWP TC activity varies and how the climatic factors affect it. It has been revealed that the TC activity over the NWP varies on annual and decadal timescales[1~3]. There are mainly three climatic factors that would affect TC activity, i.e. ENSO[4~8], monsoon circulation[9,10] and quasi-biennial oscillation (QBO)[11,12]. The Subtropical High[13], the Tibetan Plateau[14], and the sun spot activities[15] may also have some relationship with it. The locations of TC formation will change as the ENSO phase varies. The annual mean position of TC will shift eastward or westward during El Nino or La Nina phases, respectively. This adjustment can be explained by the activities of monsoon trough in the lower atmosphere[16]. During the El Nino phase, the monsoon trough moves eastward, resulting in that the vortices caused by wind shear in the lower atmosphere will increase over the southeast part of NWP. On the other hand, during the La Nina phase, the monsoon trough retreats westward, making the region of high frequency of TC formation move to the northwest part of NWP[17]. Therefore, the forward and backward movement of monsoon trough will lead to the eastward or westward swing motion of the mean location of TC formation. In addition, the QBO and Madden-Julian Oscillation (MJO) can also influence the TC activity mainly through variations of the zonal wind.

E-mail: qianwh@pku.edu.cn

The TC tracks and formation location are changed because the large scale circulation in the atmosphere has altered its location and strength under the background of greenhouse gases. Finally, these changes will influence the TC landfall activity. By now, many studies on TC landfall activity have been made in China. For example, Ye et al.[18] studied the characteristics of interdecadal variations of TC landfall on China. Zhang[19] disclosed the relationship between the frequency of TC landfall in China and the annual and decadal variations of the summer atmospheric circulation, visible heating sources and water-vapor sinks over east Asia. Tang et al.[20∼22] studied the characteristics of TC landfall on Guangdong, Huanghai-Bohai and Guangxi etc. All these results did not reveal the feature of latitudinal and longitudinal discrepancy. Lei[23] discussed how the β effect influences the characteristics of latitudinal distribution of TC landfall, but did not show the feature of TC landfall activity. Therefore, we will study the temporal and spatial characteristics of TC impact on the China mainland during the last half century. Firstly, we will introduce the data set and the methods used in this paper, then explore the climatic features and spatial distribution of TC formation over the NWP/SCS and landfall on the China mainland, and finally give the conclusions.

2 DATA AND METHODS

The TC dataset used in this article is the Best Tracks dataset obtained from JTWC (Joint Typhoon Warning Center), which includes TC signature numbers, positions observed every 6 hours, central maximum wind speed and pressure. The pressure data is not used in this study because there was no record of pressure before 1999. According to the central wind speed, TC can be divided into three classes: tropical depression (TD, with maximum central wind speed $\leq$34kn or 17m/s), tropical storm (TS, 34∼64kn, 17∼32.6m/s) and severe tropical storm (more than 64kn, 32m/s). In this study, we will neglect their discrepancies and regard them all as TC. The data spans from 1945 to 2002, including the SCS (90°E∼122°E) and the NWP (122°E∼180°E). The tracks are interpolated into 2 by 2 grids to get the passing frequencies of each grid, which can be viewed as a representation of its adjacent areas.

The methods of Rotated Empirical Orthogonal Function (REOF) and Wavelets analysis are employed to study the spatial and temporal characteristics of TC activity. The Empirical Orthogonal Function (EOF) analysis is extensively used in the field of meteorology and oceanography[24∼27], while EOF has it own deficiency[28]. The REOF can compensate the inaccuracy of EOF by most extensively revealing the modes with distinct physical meaning[29]. The method of REOF is employed in this study because the formation location and landfall site of TC have notable regional characteristics, which are caused by different environmental factors and terrain in situ. Similarly, the global wavelet spectrum analysis is used to display the temporal features of time series on different timescales[30,31].

3 CLIMATIC CHARACTERISTICS OF TC FORMATION

There are 1698 TCs generated over the NWP and the SCS during the past 58 years (1945∼2002), among which 14.25%, 242 TCs, are generated from the SCS, and 85.75%, 1456 TCs are from the NWP. On average, there are 29.3 TCs formed over the NWP and the SCS every year, among which 4.2 TCs are from the SCS and 25.1 TCs are from the NWP. Fig. 1 shows the spatial distribution of TC. Four high frequency centers are indicated by the shaded areas, one of which is located in the SCS, the other three are in the east of Philippine Sea. Gray[32] pointed out that the high sea surface temperature (SST) and large coriolis force are the basic conditions that favor the TC formation. It can also be disclosed by Fig. 1 that the areas of high frequency of TC formation are near warm pool and there are no TC formed near equator or the north of 30°N. The high frequency center of TC landfall is at the west and the north of the high frequency center of TC formation (Fig. 1 solid line).

The normalized time series of TC formation over the SCS, the NWP, both (SCS+NWP) and the TC landfall (Fig. 2(a∼d)) are used to study their temporal characteristics. Long-term linear trends indicate that the generation frequency of TC over the NWP and the SCS, as well as the TC landfall frequency in China are increased at different rates, which are consistent with the global warming[33]. The TC activities over the SCS and the NWP have decadal variation (thick solid line in Fig. 2). The accumulative anomalies show that the total amount of TC formation have distinct decadal variations, and three transition points are found near the years 1960, 1970 and 1990. While, the frequency of TC landfall does not show obvious decadal variations, which is also indicated by wavelet analysis. A ten-year time-scale transition of frequency channel can be observed from the wavelet analysis, but is not significant at the 5% level (Fig. 3b). There are 3~4 and 6~7 years oscillation before 1980, while 4~6-year oscillation appears after 1980. Two peak values are shown from global wavelet spectrum analysis with the peak of 3~7-year spectrum, passing the red noise significance test.

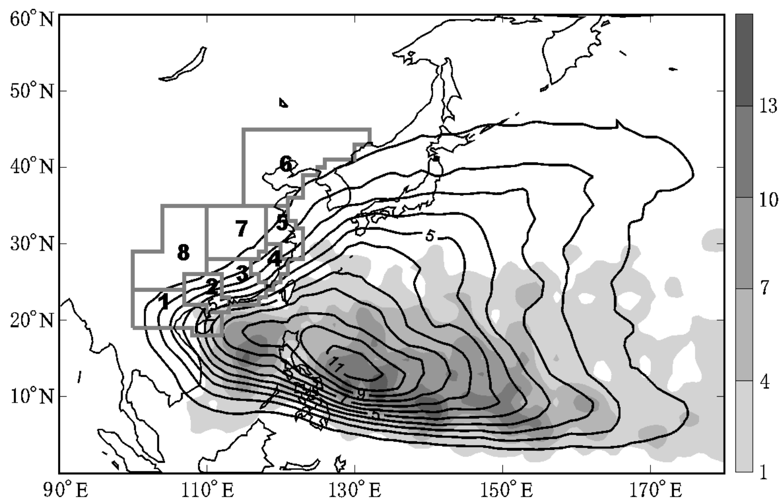

Fig. 1 Total number of tropical cyclone formation over the NWP and the SCS during the period 1945~2002 (shaded area, times/58a); the annual mean frequency of tropical cyclone passing (solid line, times/a); and regional division of the China mainland marked by rectangles with 8 numbers

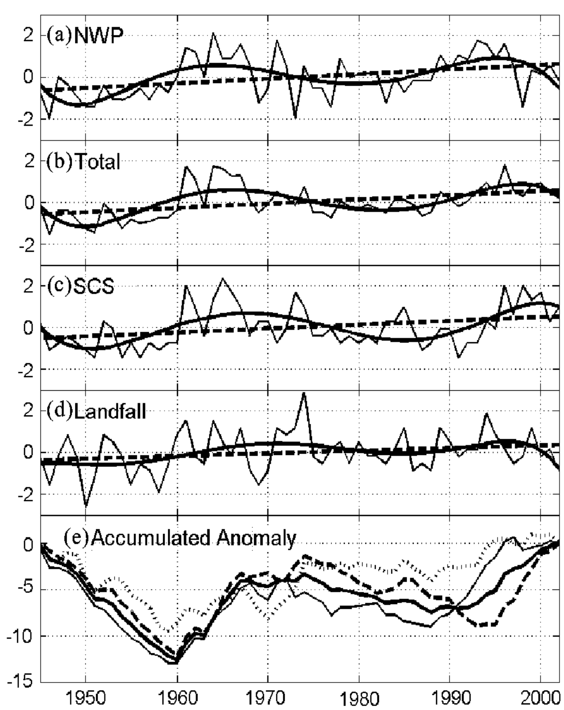

Fig. 2 Frequency of tropical cyclone formation over (a) the NWP, (b) total (the NWP and the SCS), (c) the SCS, and (d) the frequency of cyclone landfall in the China mainland

The solid line, the dashed line and the smoothly curve from (a) to (d) denote annual sum numbers, trend, and the 6- order polynomial fit, respectively. (e) The thin solid line, the thick solid line, the dashed line and the dotted line indicate the accumulated departures of tropical cyclone activity based on anomalous values of various frequencies, respectively.

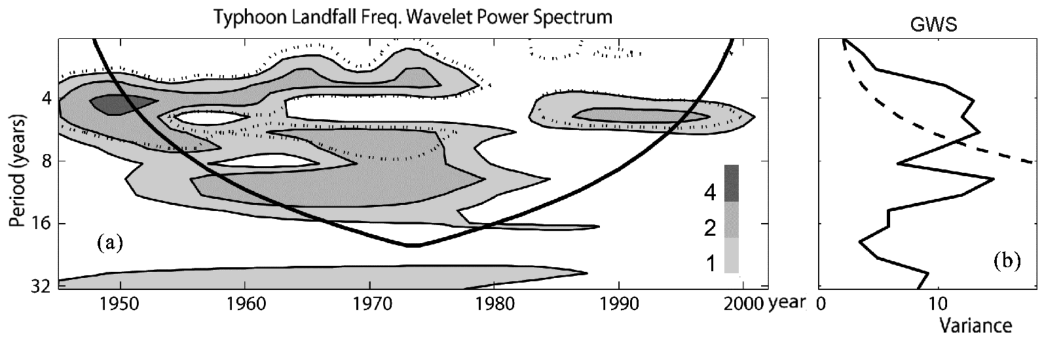

Fig. 3 Wavelet analysis for landing tropical cyclones in the China mainland during the period 1945∼2002

(a) The regions enclosed by dot lines denote passing the red noise significance at the 5% level, the thick solid line represents the boundary effect, the shaded contours represent variances.

(b) The abscissa denotes variances, the ordinate denotes the Fourier period (in year), the solid line represents the global wavelet spectrum and the dashed line represents the mean red noise spectrum.

4 SPATIAL-TEMPORAL DISTRIBUTION OF TC LANDFALL ON THE CHINA MAINLAND

4.1 General Characteristics

Totally, 439 landfall TCs on the China mainland were observed during 1945∼2002, with the 7.6 landfall TCs per year on average. There were 16 landfall TCs in 1974, reaching the maximum yearly number in history, while no landfall TC in 1950. Most TCs that landed the China mainland formed over the NWP. There were large annual number fluctuations of landfall TCs from the NWP, with the maximum of 12 TCs in 1974 and minimum of 1 TC in 2002. The interannual variations of landfall TCs from the SCS are also obvious. There were more landfall TCs during the late 1970s and after 1990, while seldom around 1970 and 1990 (Fig. 4b).

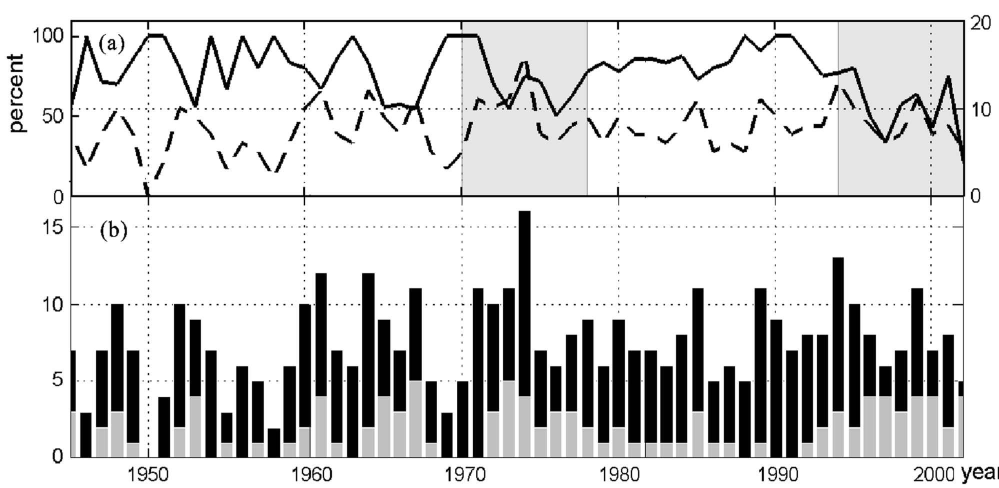

Fig. 4 Annual variations of forming tropical cyclones over the NWP and the SCS and landing tropical cyclones in the China mainland

(a) The ratio of the amount of landfall tropical cyclones formed over NWP to the total amount of landfall tropical cyclones (solid line) and the total amount of landfall tropical cyclones (dashed line). (b) Time series of tropical cyclones landed in the China mainland including those formed over the SCS (gray bars) and the NWP (black bars).

Although the total amount of landfall TCs did not change significantly in the past 30 years, those from the NWP decreased in the last 7∼8 years (Fig. 4a). As shown in Fig. 4a, there are negative correlation between the total amount of landfall TCs and the proportion of those from the NWP, with the correlation coefficient of –0.23, which is at the 10% significant level but not at 5% level. This coefficient can rise to –0.47 at the 1% significant level, if some years with shaded areas are omitted in Fig. 4. Therefore, it can be concluded that annual total sum of landfall TCs is proportional to that of coming from the SCS.

4.2 Latitudinal and Seasonal Variations of Landfall TC

The TC tracks will be different under varied atmospheric circulation, and depend on their formation location to some extent[34]. Therefore, it will help us accurately predict TC climate that we extensively study the landfall TCs at different latitudes and periods. China has a long coast line with wide span of latitude. 15 round areas, with radius of 2.5 degrees of latitude centered by 15 dots along the coast line, are chosen to represent the coastal regions at different latitudes (Fig. 5). According to the following formula, the daily sums of TC passing each representative area in 58 years are counted:

$$S_{ij} = \sum_{y=1}^{58} f_{ijy} \quad (j = 1, \cdots, 365;\ i = 1, \cdots, 15),$$

where y represents year, j is the day number in a year, i is the region serial number, f is 1 when TC passed at "i" day of "y" year, is 0 when no TC passed, and S is the sum of daily TC passing in the whole 58 years.

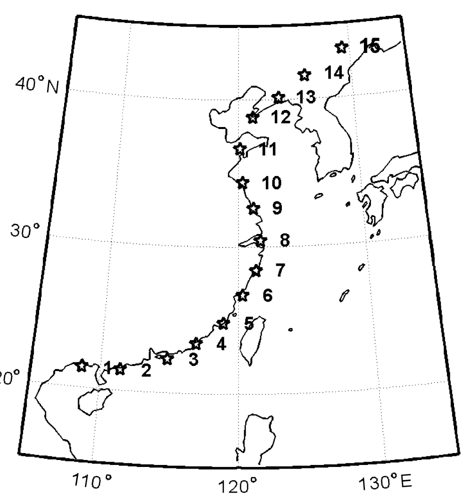

Fig. 5 Fifteen dots indicated by numbers are chosen to represent 15 different districts along the China coastlines and borders

Figure 6b shows that the number of TCs that pass region 1 is less than that of the other regions. TCs from the NWP identically affect the regions ranging from No.2 (18°N) to No.6 (27°N), indicating that the probability of TC passing the coastal region between 18°N∼27°N is consistent at different latitudes due to the westward migration of TCs. The landfall TC frequency decreases from region 6 (27°N) to region 7 (28°N). It indicates that the TC tracks turn their

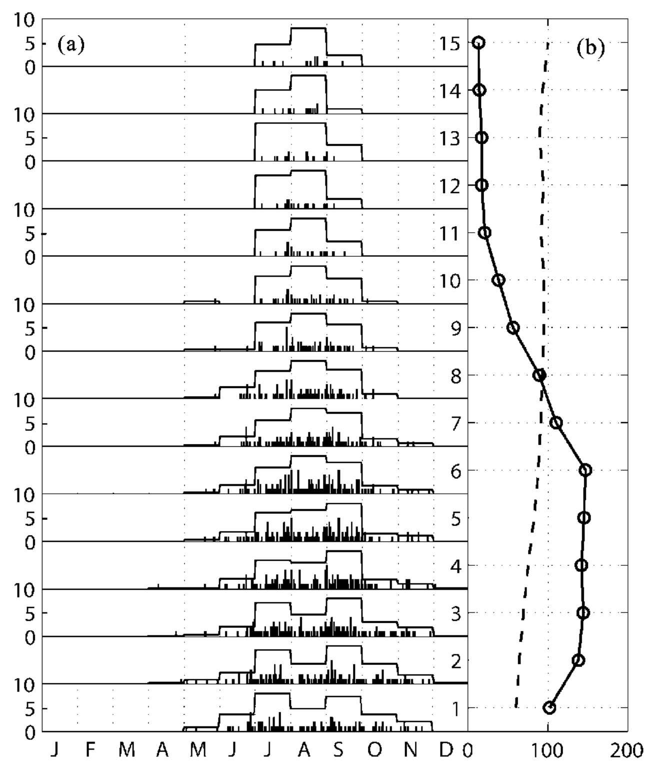

Fig. 6 Impact of the tropical cyclones formed over the NWP on the China mainland

(a) Daily (tiny bars) and monthly (bar profiles) distribution, bottom axis is month, left axis is the times of tropical cyclone landfall during the 58 years, the numbers along right axis correspond to the ones shown in Fig. 5. (b) The landfall total amount of tropical cyclones originated from the NWP (solid line), and its ratio to the total amount of tropical cyclone landfall (dashed line).

direction more frequently in this area. Meanwhile, the influence of latitude on the TC track can be certificated from the phenomena that TC passing frequency decreases quickly from region 7 to region 11. In addition, as moving northward, the proportion of the total sum of landfall TC made up by TC from the NWP steadily increases from 60% in the region 1(18°N) to 90% in the region 7(27°N). Similarly, the number of TCs from the

SCS that pass region 1 is also less than that of the other regions, and decreases from region 2 to region 7. There are seldom TCs from the SCS passing regions at high latitudes. Only 2 TCs have passed the regions higher than region 9 (33°N) in the past 58 years.

As well as the spatial differentiation of landfall TCs, there are also temporal differentiations of landfall TC in different regions. TCs from the NWP most possibly land the areas of lower latitudes represented by regions 1∼4 during June-October, and its seasonal variations exhibit bimodal distribution with two peaks in July and September. The areas at mid or high latitudes represented by regions 6∼15 have unimodal seasonal distribution with the peak in July. Region 5 also has unimodal distribution but with peak in September (Fig. 6a, solid line). All these phenomena indicate that TCs from the NWP move westward most easily in July and September, northward in August. The region 5 is the transition point of two different representative tracks.

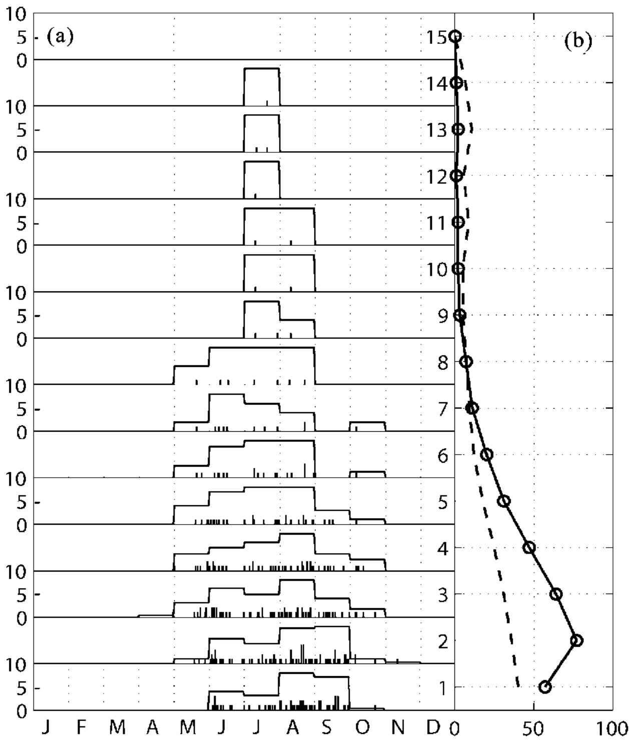

Fig. 7 Same as Fig. 6 but originated from the SCS

Figure 7a shows the temporal distribution of TCs from the SCS that pass each subregion. The landfall of TCs from the SCS is less regular than those from the NWP. The seasonal variations of landfall TCs show that there are weak bimodal distributions in regions 1∼3, and nearly unimodal distribution in the north of region 4. TCs land the areas north to region 9 mainly in July and August. From the daily distribution, it can be discovered that the highest frequency of landfall TCs from the SCS concentrated in late May and early June, and mainly regions 1∼8 are affected. There is no landfall TC which formed over the SCS in middle and late June.

After comparing the landfall TCs from the NWP with that from the SCS, we find that the landfall of TCs which are from the NWP mainly occur during July to October, while those from the SCS mainly during June to September. The seasonal distributions of two categories are similar, with bimodal distribution at lower latitudes and unimodal distribution at high latitudes. TCs from the NWP seldom affect the areas at low latitudes in August, and those from the SCS in July.

4.3 Spatial Characteristics of Landfall TC

TCs can influence the nearly half region of the China mainland, and mainly are concentrated in the eastern part. TCs land more frequently in coastal regions and the southeastern part of China; and the contour lines of landfall frequency show southwest-northeast distribution. As REOF can most extensively reveal the modes with distinct physical meaning, the former 6 modes (not shown in figures) are employed to divide the areas in the China mainland that is affected by TCs in 8 subregions (Fig. 1), among which No.1∼6 reside in the coastal region and No.7,8 inland. Fig. 8 shows the normalized time series of landfall TC frequency in different regions. The long-term trends indicate that the landfall frequency in region 7 decreases, while the frequencies in other regions increase slightly at a smaller rate than that of total landfall frequency.

Figure 8b shows the seasonal distribution of landfall TC in different subregions, in which regions 1 and 4∼8 show unimodal distribution with peak values in August, and the region 2 bimodal distributions with two peak values in July and September. Region 3 has unique distribution with almost uniform values in July, August and September. The TCs influence coastal regions and those at low latitudes in a wide time span, while inland regions and those at high latitudes in a shorter time-span.

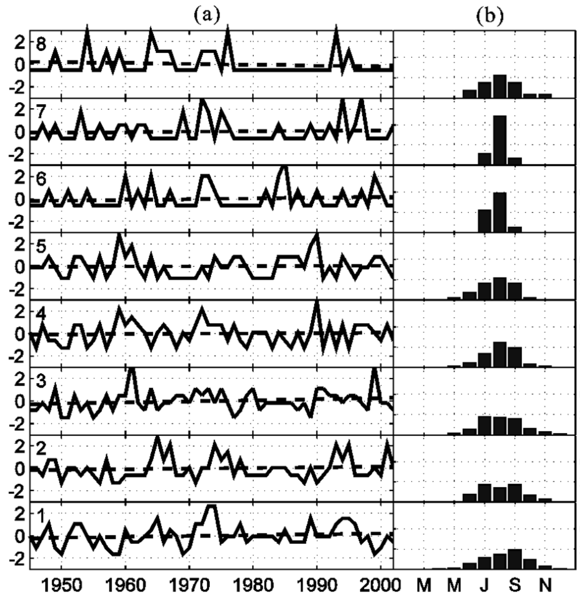

Fig. 8 Normalized time series (a) for the annual frequencies of tropical cyclone landfall over 8 areas shown in Fig. 1, and their seasonal (monthly) variations (b)

(a) Abscissa represents year, ordinate is the normalized value.

(b) Abscissa is month, ordinate is the ratio of the landfall number in each month to total amount of the area.

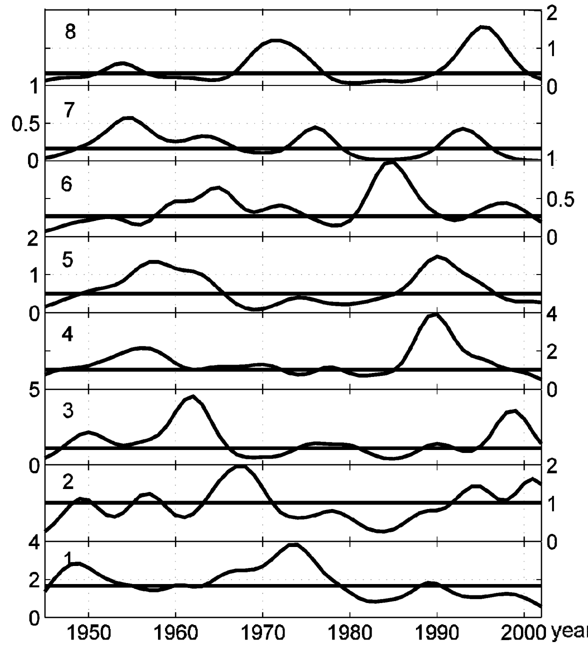

Fig. 9 Summed coefficients of the wavelet spectrum from timescales between 2 and 7 years

Numbers along the left axis represent the corresponding areas shown in Fig. 1.

There are different temporal variations of landfall TCs in different subregions. The extreme year with high or low frequency of landfall TCs changes for varied regions. From the GWS analysis (not shown in figures), it is found that the most significant spectrum is in 2∼7 years, although there are different significant periods for different subregions. This main period is probably related to ENSO cycle.

Figure 9 shows the time series filtered by 2∼7 years band-pass filter in the wavelet analysis tool. The results indicate that there is north-south oscillation of 2∼7 years period signal no matter along coastal or inland regions, and with an oscillation about 30 years. The oscillation signal is obvious along coastal regions before 1980 and along inland regions in the last 20 years.

5 CONCLUSIONS AND DISCUSSION

Through statistic analysis of TC impact on the China mainland during the last half century, we can draw the following conclusions:

(1) The frequency of TC formation over the NWP and the SCS, as well as landfall frequency in China is increased in the past 58 years, while it decreases in recent years.

(2) There are decadal variations in TC formation frequency and landfall frequency. Three transition points of the decadal variations are found around the years 1960, 1970 and 1990.

(3) The annual number of landfall cyclones is proportional to that coming from the SCS.

(4) Along the China coast line, the highest landfall frequency of cyclones is located in the southeast coast (27°N, 120°E) and the frequency rapidly decreases northward.

(5) The wavelet analysis shows that the annual series of landfall cyclone frequency has apparent spatial differentiation and timescales, varying mainly on 2∼7 years.

There are many climatic factors that can influence the interannual and interdecadal variations of TC activities, among which the SST is one of the most important factors. SST affects frequency and location of

TC formation through altering the environmental atmospheric circulation. The timescale of the interannual variations of TC formation is in accordance with the timescale of ENSO cycle. Therefore, the interannual variation of TC formation is possibly affected by SST in the Pacific Ocean, while the interdecadal variation may be affected mainly by Pacific Decadal Oscillation (PDO). The SST in the tropical Pacific affects TC activities mainly through adjusting the location of deep convection, the intensity of cross-equator wind and the strength of westerly or easterly wind. The change of PDO mode may influence the mean location and frequency of TC formation through shifting the location of Subtropical High. All of the changes in TC formation will cause the corresponding variations of landfall TCs. However, because the physical mechanism of PDO still remains obscure, the relation between PDO and TC activities need a further study.

ACKNOWLEDGMENTS

This work was supported by the National Natural Science Foundation of China (40475032,40345026).

REFERENCES

[1] Chan J C L, Shi J E. Long-term trends and interannual variability in tropical cyclone activity over the western North Pacific. *Geophys. Res. Lett.*, 1996, **23**(20): 2765~2767

[2] Chan J C L, Yip C K M. Interannual variations of tropical cyclone size over the western North Pacific. *Geophys. Res. Lett.*, 2003, **30**(24): 2267~2270

[3] Ho C H, Baik J J, Kim J H, Gong D Y, Sui C H. Interdecadal changes in summertime typhoon tracks. *J. Climate*, 2004, **17**(9): 1767~1776

[4] Pan Y H. The tele-correlation between SST in eastern tropical Pacific Ocean and the frequency of cyclone formed over western Pacific. *Chinese Sci. Bull.* (in Chinese), 1980, **25**(21): 987~989

[5] Li C Y. The study on the influence of El Nino upon typhoon action over western Pacific. *Acta Meteor. Sin.* (in Chinese), 1987, **45**(2): 229~235

[6] Clark J D, Chu P S. Interannual variation of tropical cyclone activity over the Central North Pacific. *J. Meteor. Soc. Japan*, 2002, **80**(3): 403~418

[7] Liu K S, Chan J C L. Climatologically characteristics and seasonal forecasting of tropical cyclones making landfall along the South China coast. *Mon. Wea. Rev.*, 2003, **131**(8): 1650~1662

[8] Gray W M. Atlantic seasonal hurricane frequency, Part I, El Nino and 30mb quasi-biennial oscillation influences. *Mon. Wea. Rev.*, 1984, **112**: 1649~1668

[9] Frank W M. Tropical cyclone formation. In: A Global View of Tropical Cyclones. Washington D C: Elsberry, 1987. 53~90

[10] McBride J L. Tropical cyclone formation. In: Global Perspectives on Tropical Cyclones. Geneva: Elsberry, 1995. 63~105

[11] Gray W M, Landsea C W, et al. Predicting Atlantic seasonal tropical cyclone activity by 1 August. *Wea. Forecasting*, 1993, **8**: 73~86

[12] Knaff J A. Implications of summer time sea level pressure anomalies in the tropical Atlantic region. *J. Climate*, 1997, **10**: 789~804

[13] Gong D Y, He X Z. Interdecadal Change in western Pacific subtropical high and climatic effects. *Acta Geographica Sin.* (in Chinese), 2002, **57**(2): 186~193

[14] Chen W Y, Jin D S, Wen B, et al. The influence of the winter and spring snows in Qing-Zang Plateau on the general circulation and its relation with the tropical cyclone activity. *Marine Forecasts* (in Chinese), 1997, **14**(2): 1~6

[15] Mao Z S, Jin D S. Sunspot El Nino and typhoon activity over the Northwest Pacific Ocean. *Marine Forecasts* (in Chinese), 1996, **13**(4): 56~60

[16] Chen T C, Weng S P. Interannual variation of the summer synoptic-scale disturbance activity in the western tropical Pacific. *Mon. Wea. Rev.*, 1998, **126**: 1725~1733

[17] Wang B, Chan J C L. How strong ENSO events affect tropical storm activity over the Western North Pacific. *J. Climate*, 2002, **15**(13): 1643~1658

[18] Ye Y, Dong B. Interdecadal change analysis of the landing tropical cyclone over China. *Marine Forecasts* (in Chinese), 2002, **19**(2): 23∼30

[19] Zhang Q Y, Peng J B. The interannual and interdecadal variations of East Asian summer circulation and its impact on the landing typhoon frequency over China during summer. *Chinese J. Atmos. Sci.* (in Chinese), 2003, **27**(1): 97∼106

[20] Tang X C, Liu H P, Pan A D, et al. Analysis of Disastrous features of landing typhoon in coastal regions of Guangdong province in recent 50 years. *Sci. Geographica Sin.* (in Chinese), 2003, **23**(2): 182∼187

[21] Zhang X H, Lu X, Yan M. The statistical characteristic analysis of the influence of the tropical cyclones on the Yellow sea and the Bohai sea. *Transactions of Oceanology and Limnology* (in Chinese), 2003, **2**: 11∼16

[22] Wu X G. The statistical characteristic analysis of the influence of the tropical cyclone on Guangxi province in recent 50 years. *J. Guangxi Meteo.* (in Chinese), 1998, **19**(4): 28∼30

[23] Lei X T, Chen L S. The latitudinal distribution of climatic characteristics on tropical cyclone activities in the WNP. *J. Applied Meteo. Sci.* (in Chinese), 2002, **13**(2): 218∼227

[24] Saji N H, Goswami B N, et al. A dipole mode in the tropical Indian Ocean. *Nature*, 1999, **401**: 360∼363

[25] Sterl A, Hazeleger W. Coupled variability and air-sea interaction in the South Atlantic Ocean. *Climate Dynamics*, 2003, **21**(7-8): 559∼571

[26] Jung T, Hilmer M, Ruprecht E, et al. Characteristics of the recent eastward shift of interannual NAO variability. *J. Climate*, 2003, **16**(20): 3371∼3382

[27] Camp C D, Roulston M S, Yung Y L. Temporal and spatial patterns of the interannual variability of total ozone in the tropics. *J. Geophys. Res.*, 2003, **108**(D20): 4643

[28] Dommenget D, Latif M. A cautionary note on the interpretation of EOFs. *J. Climate*, 2002, **15**: 216∼225

[29] Qian W H, Hu H R, Zhu Y F. Thermocline oscillation and warming event in the tropical Indian Ocean. *Atmosphere-Ocean*, 2003, **41**(3): 241∼258

[30] Torrence C, Compo G P A. Practical guide to wavelet analysis. *Bull. Amer. Meteor. Soc.*, 1998, **79**(1): 61∼78

[31] Qian W H, Chen D, Zhu Y F, et al. Temporal and spatial variability of dryness/wetness in China during the last 530 years. *Theoretical and Applied Climatology*, 2003, **76**(1-2): 13∼29

[32] Gray W M. Global view of origin of tropical disturbances and storms. *Mon. Wea. Rev.*, 1968, **96**: 669∼700

[33] Knutson T R, Tuleya R E. Increased hurricane intensities with CO_2-induced warming as simulated using the GFDL hurricane prediction system. *Climate Dyn.*, 1999, **15**(7): 503∼519

[34] Chen L S, Xu X D, Luo Z X, et al. Introduction to Tropical Cyclone Dynamics (in Chinese). Beijing: China Meteorological Press, 2002